

# Stability of cool flux tubes in the solar chromosphere

## II. Non-linear dynamical behaviour

S.S. Hasan<sup>1</sup> and F. Kneer<sup>2</sup>

<sup>1</sup> Indian Institute of Astrophysics, Sarjapur Road, Bangalore 560 034, India

<sup>2</sup> Universitäts-Sternwarte, Geismarlandstrasse 11, D-3400 Göttingen, Federal Republic of Germany

Received September 21, accepted November 22, 1989

**Abstract.** The present investigation is a continuation of earlier work (Hasan and Kneer, 1986) on the stability of cool flux tubes in the solar chromosphere. We focus our attention on a single vertical flux tube, which we assume to be in pressure and thermal equilibrium with the external field free medium. For the ambient medium we consider a model atmosphere in radiative and hydrostatic equilibrium. Owing to the presence of carbon monoxide, there exists a region, at a height of some 650 km above optical depth unity, where the temperature gradient is super-adiabatic. This drives a convective instability. The time evolution of this instability is followed by solving the MHD equations in the thin flux tube approximation. Energy exchange with the radiation field is included in the analysis. During the first few hundred seconds, large amplitude chaotic motions are generated. Subsequently, overstable oscillatory motions are set up, with a period of around 200 s. In the top layers of the model ( $z \approx 1500$  km), the amplitudes of the temperature and velocity fluctuations are 1500 K and  $4\text{--}5 \text{ km s}^{-1}$  respectively. Our simulations of a flux tube, with a transmitting upper boundary, show that the average energy flux in the oscillations is inadequate for chromospheric heating. However, the oscillations reveal several interesting features, which are noteworthy in themselves.

**Key words:** hydromagnetics – Sun – chromosphere – convective and radiative instabilities – nonlinear dynamics

### 1. Introduction

In the first paper of this series (Hasan and Kneer, 1986, hereafter designated as Paper I), we investigated the dynamic stability of a solar atmospheric model, threaded with a vertical magnetic field. Owing to the presence of carbon monoxide (CO), there exists a low temperature region ( $\approx 2000$  K) in the model at a height of about 650 km above  $\tau_{5000} = 1$ . The temperature gradient at this height is steep enough to render the atmosphere convectively unstable. Using a linear analysis, we showed in Paper I, that below a critical value of the magnetic field strength, purely convective modes occur, whereas for stronger fields, the instability takes the form of overstable oscillations, similar to sub-photospheric flux tubes (Hasan, 1985, 1986, 1989).

Send offprint requests to: S.S. Hasan

Investigations into the CO cooling problem have recently attracted interest as well as some controversy. In general, much attention has been focused on molecule formation in the atmospheres of cool stars, with a view to obtaining a clearer understanding about the structure of their outer layers. It was recently suggested by Kneer (1983, 1984, 1985) that molecular radiative cooling may lead to mechanical heating of the upper atmosphere, thus producing a chromosphere. Muchmore et al. (1987) and Tsuji (1988, 1989) pointed out the consequence of the low temperatures and instabilities on dust formation and stellar wind dynamics.

As far as the outer solar atmosphere is concerned, Ayres et al. (1986) found from low spatial and high spectral resolution observations of the Ca II K-line and the CO IR rotation-vibration bands, conflicting high and low temperatures. They reconciled this apparent disparity by invoking multi-column models and concluded that “the chromosphere of the Sun is highly structured”, in agreement with the observations of Secchi (1877). From a time-dependent numerical simulation, Muchmore et al. (1988) calculated equilibrium models with CO cooling and found that in general different atmospheric structures are possible. Their equilibrium models are very similar to those of Kneer (1985), with an outer temperature close to 2000 K. Thermally bifurcated states i.e., two different radiative equilibrium (RE) models with the same effective temperature found earlier by Kneer (1985) and Muchmore (1986), is also reproduced in these models.

While earlier investigations (e.g., Kneer, 1983, 1985; Muchmore et al., 1988) took into account only few atomic lines in addition to H<sup>-</sup> and CO for the construction of the equilibrium models, an important step forward was made by Anderson (1989). He included practically all the important lines to calculate a line blanketed RE model in non-LTE, with an outer temperature close to 2600 K. It is worth noting that at such temperatures, other molecular species can form, reducing the temperature still further. Anderson predicted from his model that mild convection in the CO cooled layers would occur, leading to a decrease in the temperature gradient. Convection was indeed found in the numerical simulations of Steffen and Muchmore (1988). The reaction of RE models with CO cooling upon non-radiative energy supplied from outside the atmosphere was investigated in a parameterised fashion by Kneer (1985) and Anderson and Athay (1989) and in a more sophisticated manner by Muchmore et al. (1988), using acoustic wavetrains. The results of all these analyses are similar and confirm that increasing the supply of input energy

tends to inhibit the formation of a CO cooled region until finally a pure chromospheric temperature rise is produced.

In the present investigation, we approach the CO radiative instability from a different point of view. It is well known from observations that the photospheric field occurs in the form of discrete magnetic elements. Even in the chromosphere it is likely that the inhomogeneous nature of the field will be preserved. We focus our attention on the development of the instability in a vertical flux tube and address the question: Is it possible for the chromosphere to be self-excited by an instability located within the atmosphere itself? Can dynamical processes transport energy from the unstable region to higher layers and dissipate it there to form a chromosphere? The linear stability of a RE atmosphere, with CO cooling, in a flux tube, was examined in Paper I. However, a linear analysis is not appropriate for determining the amplitudes of the motions and calculating the amount of energy transported due to dynamical processes. This is because nonlinear effects are important in the atmosphere, particularly in the upper layers, in view of the small pressure scale height. For this reason, we resort to a nonlinear treatment of the MHD equations.

Similar to Paper I, we work within the framework of the thin flux tube approximation for reasons of mathematical tractability. For the same reasons, we do not take full account of the complexities in the multi-line non-LTE approach, such as those treated by Anderson (1989). Rather, our aim is to extend the analysis of Paper I to treat nonlinear effects and to see how they affect the dynamics and energy transport in the atmosphere. Further refinements to the model will be undertaken in subsequent investigations. The plan of our paper is as follows: in the following section, we describe the initial RE model and outline the method used in solving the MHD equations along with the boundary conditions. In Sect. 3, we present the results of the simulations and finally in Sect. 4, we discuss the main findings and summarise the conclusions of our study.

## 2. Model and mathematical formulation

### 2.1. Initial model atmosphere

We start from the RE model described in Paper I, for the unmagnetised atmosphere outside the flux tube. We consider a vertical extension from  $z = 80$  km, where  $z$  measures the height above  $\tau_{5000} = 1$ , to  $z = 1640$  km and furthermore assume the atmosphere to be in hydrostatic and radiative equilibrium with  $T_{\text{eff}} = 5950$  K. The reason for using an effective temperature about 170 K higher than the solar value is given in Paper I. Absorption and emission of radiation occurs through  $\text{H}^-$  bound-free and free-free transitions and CO line transitions in the fundamental rotation-vibration band ( $\Delta v = 1$ ) at  $\lambda = 4.6 \mu$ . Both  $\text{H}^-$  and CO populations are assumed to be in LTE, and radiative transfer is treated in the Eddington approximation. For the CO line transfer, opacity distribution functions (ODF) are used. The model exhibits a dip in the temperature structure about 150 km wide at  $z = 700$  km, as can be seen in Fig. 1. At  $z = 650$  km, the temperature drops from nearly 4800 K to some 2000 K, due to strong cooling by CO, when the optical depth in the CO lines becomes small ( $\tau_{\text{CO}} < 1$ ). We have chosen this model atmosphere for its extreme temperature stratification. The temperature in the region dominated by CO cooling is so low that  $\text{H}_2$  molecules form and consequently, the RE temperature gradient becomes superadiabatic, very much in the same way as it does in the subphotospheric layers.

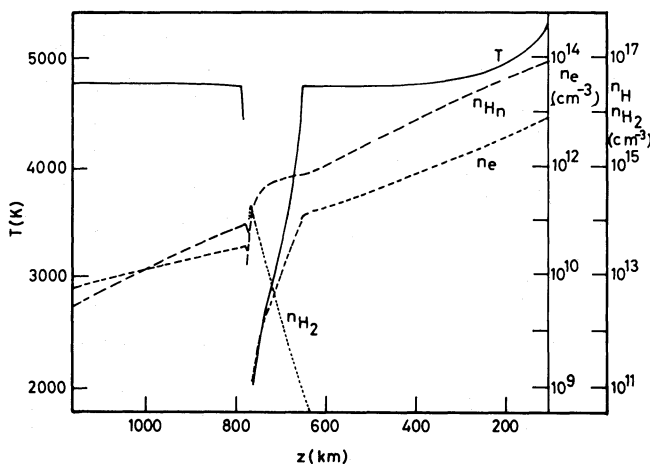


Fig. 1. The variation of  $T$ ,  $n_e$ ,  $n_{\text{H}}$  and  $n_{\text{H}_2}$  with  $z$

At this point, a comment on the use of ODF for the CO rotation-vibration transitions is appropriate. This was criticised by Mauas et al. (1989), who performed frequency by frequency calculations for a total of 2220 lines of the CO IR fundamental band to obtain the net radiative losses by CO molecules in semi-empirical models. We consider this criticism to be unjustified, although ODF admittedly do have their weaknesses (Mihalas, 1978). Mauas et al. do not in fact compare their CO cooling results with calculations using ODF, but rather extend earlier estimates (such as those of Ayres, 1981 or Kneer, 1983) based on one-point frequency quadratures for the optically thin (cooling) case to high opacity, density and temperature regimes. In the latter, the approximate formulae cannot apply. Contrary to their claim, Mauas et al., in fact, demonstrate (cf. their Table 3 and Fig. 6) that at low optical depths, the CO formation is autocatalytic i.e., increases strongly with decreasing temperature.

We assume that the temperature in the flux tube at the initial instant is the same as that in the ambient medium. The internal pressure is determined by invoking horizontal pressure balance, such that

$$p(z) + \frac{B^2}{8\pi} = p_e(z) \quad (1)$$

where  $p$  and  $p_e$  are the internal and external pressures respectively and  $B$  is the magnetic field. We can rewrite Eq. (1) as

$$p(z) = \frac{\beta}{\beta + 1} p_e(z) \quad (2)$$

where

$$\beta = \frac{8\pi p}{B^2}. \quad (3)$$

At the initial instant we choose  $\beta$  to be constant with height in the atmosphere, which implies that the pressure (as well as density) in the flux tube is lower than the external value by a constant factor at each height. This atmosphere is, of course, no longer in radiative equilibrium.

### 2.2. Equations

The time evolution of the atmosphere is now followed within the framework of the thin flux tube approximation (Defouw, 1976;

Roberts and Webb, 1978). As already stated in Paper I, this approximation in the present context, is taken to the limit of its applicability, since in the upper layers of our model, the tube radius is no longer smaller than the pressure scale height. Nevertheless, we still use it for mathematical convenience, since the equations in this approximation are one-dimensional.

The equations we employ are essentially the same as those used in Hasan (1984), apart from the energy equation, which is

$$\rho C_v \left( \frac{\partial T}{\partial t} + v \frac{\partial T}{\partial z} \right) = -\rho C_v (\gamma - 1) T \Delta \frac{\chi_\rho}{\chi_T} + \rho \dot{Q} \quad (4)$$

where  $t$  denotes time,  $\rho$  is the mass density,  $T$  is the temperature,  $v$  is the vertical component of velocity,  $\Delta = (\nabla \cdot \mathbf{v})_{r=0}$ ,  $C_v$  is the specific heat at constant volume,  $\gamma$  is the ratio of specific heats,  $\chi_T = 1 - (\partial \ln \mu / \partial \ln T)_\rho$ ,  $\chi_\rho = 1 - (\partial \ln \mu / \partial \ln \rho)_T$ ,  $\rho \dot{Q}$  is the radiative energy loss per unit volume, and is given by

$$\rho \dot{Q} = 4\pi \int_0^\infty \kappa_\nu (S_\nu - J_\nu) d\nu. \quad (5)$$

In LTE, the source function  $S_\nu$  is the Kirchhoff-Planck function  $B_\nu(T)$ ,  $J_\nu$  is the mean intensity and  $\kappa_\nu$  is the absorption coefficient. The integral in Eq. (5), over frequency  $\nu$ , is approximated by a sum with appropriate summation weights (cf. Paper I). The calculation of  $J_\nu$  is in general rather complicated, since the equation of radiative transfer is two dimensional. However, considerable simplification occurs if we treat the problem in either the optically thin or optically thick limits. In the former, the tube is assumed transparent to all radiation, and the radiation intensity in the flux tube is equated to the external value. On the other hand, in the opposite extreme, we assume that the flux tube builds up its own radiation field and  $J_\nu$  is calculated as for the initial plane parallel external atmosphere, using the equation

$$\frac{1}{3} \frac{d^2 J_\nu}{d\tau_\nu^2} = J_\nu - S_\nu(T) \quad (6)$$

where  $\tau_\nu$  is the optical depth in the vertical direction, corresponding to frequency  $\nu$ .

### 2.3. Numerical method

Equations (1) and (4) along with the equations of continuity and motion [Eqs. (1) and (2) in Hasan, 1984] were solved numerically using the flux corrected transport (FCT) scheme of Boris and Book (1976). This is an explicit finite difference scheme, with second order time accuracy. Starting from the initial static model atmosphere, described in Sect. 2.1, the equations were integrated forward in time. The transfer equation was solved at each time step, using the instant values of the thermodynamic variables. The pressure was calculated via the ionisation (and molecular dissociation) equilibrium, which were assumed to be achieved instantly. We also assumed all atomic and molecular species to be in LTE, except hydrogen, for which we employed an analytic expression for the departure coefficients (Kneer and Mattig, 1978 and Paper I).

A uniform spatial grid consisting of 157 pt was used in the computations. With lower and upper boundaries at  $z = 80$  km and  $z = 1640$  km respectively, this gave a grid size of 10 km. The time step was chosen small enough to satisfy the Courant Friedrich Levy criterion, which typically yielded a value in the range 1–2 s.

### 2.4. Explicit vs. implicit treatment of radiative exchange

It was not obvious to us a priori, whether an explicit treatment of the radiative loss term in Eq. (4) was justified, in view of the nonlocal nature of the radiation field. In order to check this, we performed another calculation in which this term was treated implicitly. The temperature was first calculated explicitly using FCT on Eq. (4), without  $\dot{Q}$ . Denoting this value as  $T_h$ , the final temperature with radiative loss was calculated by solving

$$\frac{\partial T^{(n+1)}}{\partial t} = \frac{\partial T_h^{(n+1)}}{\partial t} + \frac{\dot{Q}^{(n+1)}}{C_v}$$

where the index  $n+1$  refers to values at the new time step (we are thankful to J. Mariska for suggesting this explicit cum implicit treatment). A comparison of the explicit and implicit calculations after  $t = 1000$  s showed minor differences. The reason for the good agreement lies in the shortness of the time step of about 1 s, compared with the radiative time scales which are of the order of  $10^2$  s or longer. Obviously, explicit computations run much faster than implicit ones, because for the latter, one has to obtain temperatures and opacities consistent with the radiation field. This requires an iterative scheme. In view of this, we chose to use the fully explicit method.

### 2.5. Boundary conditions

The treatment of boundary conditions, especially at the top boundary requires careful handling, in view of the low gas density there. For practical reasons, we consider a finite vertical extension of the atmosphere and impose boundary conditions at some height. Since there are in fact no physical boundaries, these conditions should be as ‘inert’ as possible. We chose a transmitting boundary condition for the upper boundary, when the flow in the flux tube was upwards. This condition was implemented by using the method of characteristics (Courant and Friedrichs, 1948). The characteristic equations are

$$\frac{dp_\pm}{dt} \pm \rho c_t \frac{dv_\pm}{dt} = \frac{v \rho_e g c_t^2}{v_a^2} \pm \rho c_t g + \frac{\rho \chi_T \dot{Q} c_t^2}{C_v \mu c_s^2} \text{ along } C_\pm \quad (7a, b)$$

$$\frac{dp_0}{dt} - c_s^2 \frac{d\rho_0}{dt} = \frac{p \chi_T \dot{Q}}{C_v T} \text{ along } C_0 \quad (8)$$

where  $c_s = \sqrt{\gamma p / \rho}$  is the sound speed,  $v_a = B / \sqrt{(4\pi \rho)}$  is the Alfvén speed and  $c_t = c_s v_a / \sqrt{c_s^2 + v_a^2}$  is the tube speed. The characteristic curves  $C_\pm$  and  $C_0$  are given by

$$C_\pm: \left( \frac{dz}{dt} \right)_\pm = v \pm c_s, \quad (9a, b)$$

$$C_0: \left( \frac{dz}{dt} \right)_0 = v. \quad (10)$$

At the upper boundary, only one boundary condition needs to be specified during the upflow phase, when the flow speed is less than the tube speed. We assumed that  $v$  was constant along the  $C_+$  characteristic. The remaining variables  $p$  and  $\rho$  were then determined from Eqs. (7a) and (8). When  $v > c_t$ , no boundary conditions need to be given. During the downflow phase, we kept the pressure and density constant at this boundary.

At the lower boundary, we assumed a rigid boundary and put  $v = 0$ . This is probably a reasonable choice, since the gas density is

fairly high here. We also assumed that  $\rho$  was constant. The pressure was calculated using the  $C_-$  characteristic. Further details about the numerical implementation of the boundary conditions using characteristics can be found for example in Hasan and Venkatakrishnan (1980).

In solving the transfer Eq. (6), the same boundary conditions as those used in Paper I were used. Briefly, at the upper boundary we assumed no incoming radiation from above and at the lower boundary, the radiative flux was kept constant in time at the value  $\sigma T_{\text{eff}}^4$ .

### 3. Results

It is important to note that the dynamical behaviour of the model flux tubes described in the following sections is due solely to the unstable initial stratification. RE models, in which only  $H^-$  contributes to the radiative energy exchange, exhibit hardly any motions ( $|v| < 300 \text{ m s}^{-1}$  in the top layers) when a magnetic field is introduced in the atmosphere. This small motion in general damps out after some hundred seconds.

#### 3.1. Optically thick vs. optically thin for $\beta_0 = 2$

In Fig. 2, we compare the time evolution of  $v$  at various heights for (a) the optically thick and (b) optically thin cases, assuming  $\beta_0 = 2$ . Noting that the atmosphere in the flux tube is in general not in energy equilibrium at  $t=0$ , it is hardly surprising to observe that the initial response is a large transient. During this transient phase, the atmosphere seeks to relax towards a new equilibrium. This explains the large oscillation at the very beginning in both cases for some hundred seconds or so. Subsequently, we observe that the oscillations begin to increase in amplitude, suggesting the presence of an overstability. The velocities are higher in the optically thin case, possibly because of the shorter radiative exchange time scale (as defined by Spiegel, 1957).

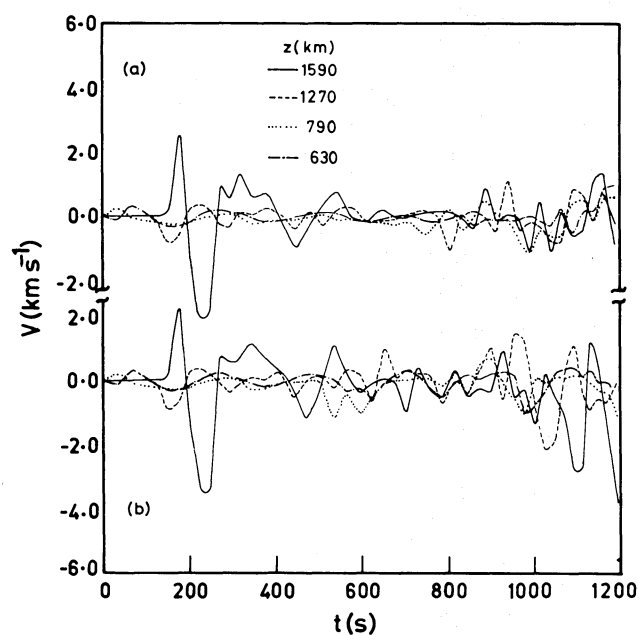


Fig. 2a and b. Time variation of  $v$  at various heights, for a optically thick and b optically thin cases for  $\beta_0 = 2.0$

(N.B. In contrast to Spiegel's formulation of radiative smoothing of disturbances, we deal with an overstable situation, where the optical thickness determines the growth rate of the amplitudes—see Paper I and also Kneer, 1986).

#### 3.2. Optically thick case for $\beta_0 = 4$

We discuss this case in some detail as a typical example of the nonlinear behaviour of a convectively unstable atmosphere (with CO) in a flux tube.

##### 3.2.1. Velocities

In the linear analysis of Paper I, we found that the instability growth rate increases with  $\beta_0$ . This is because, the magnetic field has a stabilising effect upon the instability. Thus, a decrease in the field strength, or equivalently an increase in  $\beta_0$ , should yield higher velocities. This is indeed what happens, as a comparison of Figs. 3 and 2a shows. The velocities in the upper layers can become as high as  $4\text{--}5 \text{ km s}^{-1}$ , i.e., greater than the tube speed  $\approx 3 \text{ km s}^{-1}$ . After very irregular motions during the first 350 s, an oscillation with an approximate period of 200 s is set up. The top layers need more time to come into phase with the deeper layers and their motions, which are highly nonlinear, deviate from sinusoidal perturbations.

Figure 4 depicts the height dependence of the velocity at various instants of time. It is found that the low photosphere does not take part in the motion, as the density there is much higher than that in the chromosphere. The source of the motions is the instability layer at  $z \approx 600 \text{ km}$ . After a time lapse of 800 s, the whole atmosphere moves coherently, apart from the extreme top layers, which are possibly influenced by the boundary conditions.

##### 3.2.2. Temperature

In Fig. 5, we show the time evolution of  $T$  at the same heights as for  $v$ . Denoting the peak to peak temperature deviation as  $\Delta T$ , we find  $\Delta T \approx 3000 \text{ K}$ . A comparison of the  $v$  and  $T$  curves shows that,

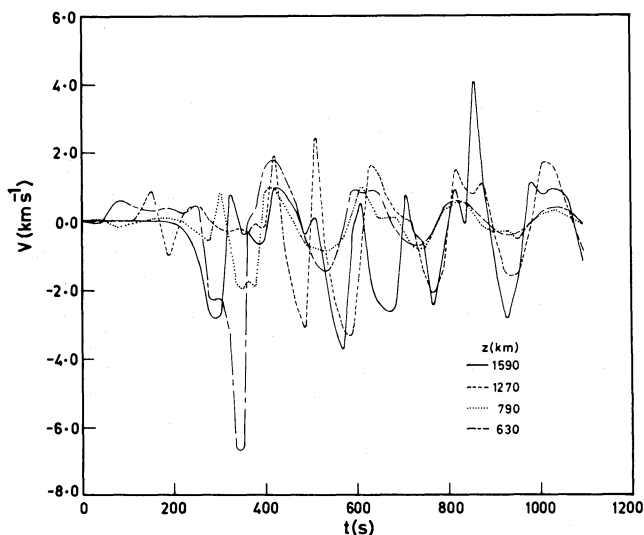


Fig. 3. Time variation of  $v$  at various heights for  $\beta_0 = 4$  in the optically thick case



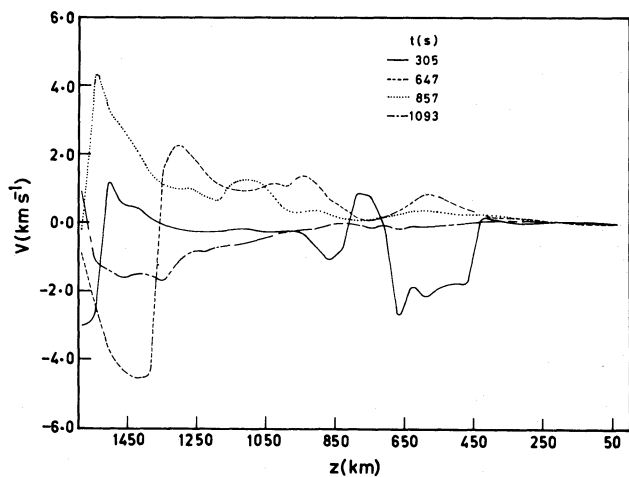


Fig. 4. Velocity as a function of  $z$  at various times in the optically thick case, for  $\beta_0 = 4$

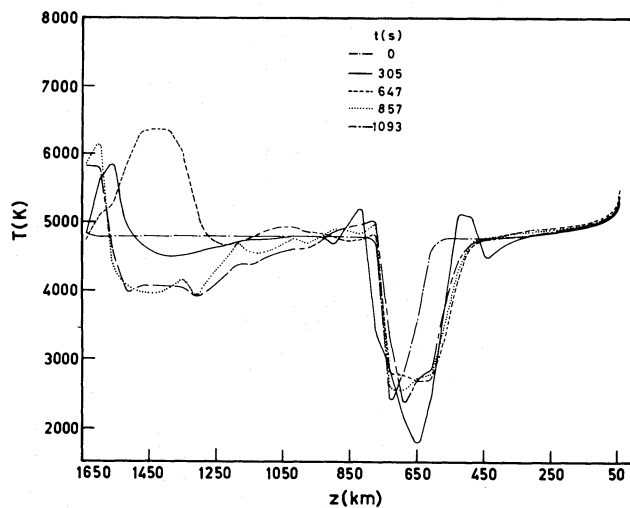


Fig. 6. Temperature as a function of  $z$  at various times for  $\beta_0 = 4$  in the optically thick case

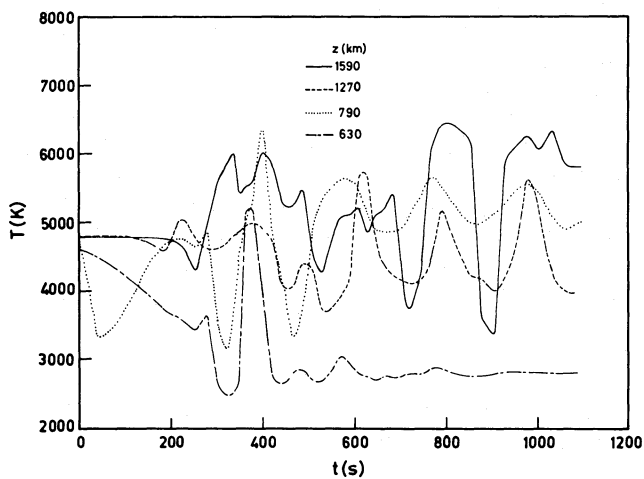


Fig. 5. Time variation of  $T$  at various heights for  $\beta_0 = 4$  in the optically thick case

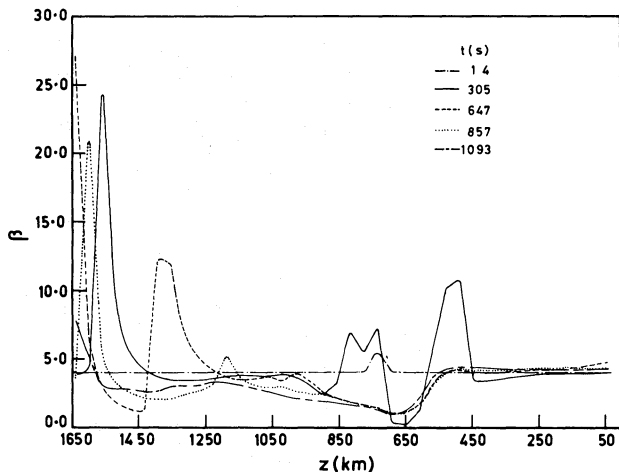


Fig. 7. Height variation of  $\beta$  at various times, for  $\beta_0 = 4$  in the optically thick case

at large  $t$ , velocity and temperature are out of phase, with the temperature leading by some 50 s.

Figure 6 depicts the  $z$  dependence of  $T$  at various elapsed times. The dash-dot curve gives the initial profile (which is the same as the external one). The temperature 'dip' at  $z \approx 600$  km widens very quickly during the initial phase and its bottom fills up as well. The abrupt temperature drop shifts downwards to  $z = 550$  km. Curiously, this is also the level at which the temperature rise in empirical models (e.g., Vernazza et al., 1981) occurs. The displacement of the temperature drop is a dynamic effect. The internal energy of the unstable layer at  $z \approx 600$  km and the radiative energy absorbed in it are responsible for driving and maintaining chromospheric motions.

### 3.2.3. Magnetic field

Our choice of  $\beta_0 = 4$  corresponds to an initial magnetic field of  $B = 590$  G at  $z = 0$  and  $B = 0.37$  G at  $z = 1640$  km. Thus, the

diameter of the tube increases from the bottom to the top by a factor 40. These field strengths are much smaller than the kG fields inferred from observations in photospheric flux tubes (e.g. Stenflo, 1973 and Wiehr, 1978).

Figure 7 depicts the height variation of  $\beta$  at various times. The dash-dotted curve corresponds to almost the beginning ( $t = 1.4$  s), when  $\beta$  is constant with  $z$ . In the higher layers,  $\beta$  undergoes strong fluctuations. These large changes are also found to occur in  $B$  and the tube diameter. However, it is interesting to note that at  $z = 600$  km,  $\beta$  settles down to values lower than the initial one, with a mean value of about 0.8 at  $z = 700$  km and a corresponding field strength of 60 G. This behaviour is an example of a 'convective collapse' in a superadiabatically stratified medium, very similar to the results obtained by Hasan (1984, 1985) in simulations of subphotospheric flux tubes. As was demonstrated in these papers, the local increase of the magnetic field, stabilises

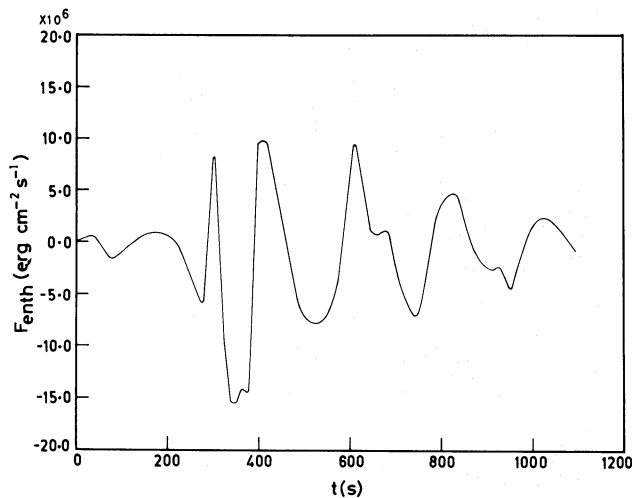


Fig. 8. Enthalpy flux, at  $z = 790$  km, as a function of  $t$ , for  $\beta_0 = 4$  in the optically thick case

Table 1. Time averaged enthalpy flux at different heights

$z$ (km)	$\langle F_{\text{enth}} \rangle$ ( $\text{erg cm}^{-2} \text{s}^{-1}$ )
630	$3.5 \cdot 10^6$
790	$-3.2 \cdot 10^5$
1270	$-2.0 \cdot 10^3$
1590	$-5.5 \cdot 10^2$

the atmosphere against dynamical instability (see also the discussion by Schüssler, 1989). The pressure in the flux tube can be calculated by using Eq. (1). In general, we find that ‘convective collapse’ in the superadiabatic layer leads to a rarefied atmosphere there with a pressure of some 40% of the external value. The pressure in the upper layers is on an average between 2–5% of the ambient value, whereas below the temperature minimum it hardly changes from its initial value  $\beta_0/(\beta_0 + 1)$ .

### 3.2.4. Energy

Inspection of the various quantities that contribute to energy transport, we find that the enthalpy flux  $F_{\text{enth}} = 5/2(n_{\text{tot}}kTv)$  is the dominant term. Figure 8 shows the variation of  $F_{\text{enth}}$  with  $t$  at  $z = 790$  km. We find that, after the initial phase, it oscillates about zero with a 200 s period. In Table 1, the time averages of  $F_{\text{enth}}$  at four heights are given (we disregard the initial transient behaviour upto 400 s for averaging).

Three of the four values in Table 1 are negative. But this has no physical significance, and for all practical purposes we can take them to represent no net enthalpy flux. Even their absolute values fall short of the energy requirements deduced from empirical solar models (Vernazza et al., 1981; Anderson and Athay, 1989). As may also be seen from Fig. 5, there is on average no significant temperature increase at high atmospheric layers. Sim-

ilar results were also obtained for other values of  $\beta_0$  and also for the optically thin limit.

## 4. Discussion and conclusions

The aim of the present study was to extend the calculations of Paper I to the nonlinear regime with a view to examining the consequences of having a self-exciting mechanism of oscillations above the photosphere. In particular, we investigated the possibility whether the motions driven by the CO instability could extract sufficient energy from the radiation field near the  $T_{\text{min}}$  region of empirical models (at  $z \approx 500$  km) and deposit it in higher layers to produce chromospheric heating. The magnetic field serves the role of guiding the waves in the vertical direction. Our results, however, indicate that the necessary heating does not occur. The temperature increase in the upper layers is not sufficient to term the final configuration as a chromosphere. What is, however, found is that an overstable oscillation with a period of some 200 s develops, with high amplitudes in the top layers, but with very little energy transport. It is possible that with a reflecting upper boundary, such as could arise due to a sharp temperature rise in a transition layer, the results may have been different. We defer the treatment of this case to a subsequent investigation. Thus, an important finding to emerge from our study is that the solar chromosphere, i.e., a non-radiatively heated atmospheric region, does not develop due to a self-exciting instability located at some 500–600 km above the photosphere, even with an extremely unstable configuration.

If the oscillations driven by the CO instability are not capable of producing the required heating to simulate the chromospheric temperature rise, the question of course arises whether there is any other process, for heating the atmosphere. Although this is beyond the scope of the present analysis, we would still like to comment on this point. Earlier work (Ulmschneider, 1970; Stein, 1967; Stein and Leibacher, 1974 and references therein) suggested that pure acoustic waves could heat the chromosphere. However, OSO-8 observations failed to confirm this hypothesis (Athay and White, 1978). On theoretical grounds also, there are reasons for doubting this. For instance Musielak and Rosner (1987, 1988) found that the earlier estimates of the energy fluxes generated in the convection zone to be too high. Heating by flux tube waves may offer more promise (Musiela et al., 1987, 1989; Ulmschneider and Zähringer, 1987), but the problem of generating an adequate energy flux still remains. It is quite possible that the energy flux necessary for chromospheric heating is produced as a combination of several mechanisms, but this aspect needs further investigation.

Even though the results of our simulations indicate that the energy flux in the overstable oscillations, excited due to the CO instability, is insufficient to meet the requirements of the chromosphere, the results nevertheless possess several interesting features. The motions which are partly chaotic and partly periodic are reminiscent of the temporal behaviour seen in H $\alpha$  in small-scale structures of the chromospheric network (e.g., Kneer and von Uexküll, 1986; von Uexküll et al., 1989 and references therein). It is somewhat fortuitous that the period of the oscillation found by us is close to the observed chromospheric 3 min mode (e.g., Orrall, 1966; Liu, 1974; Cram, 1974), which is likely to occur within magnetic flux tubes (Kalkofen, 1989). However, in view of the dependence of the oscillation frequency on  $\beta_0$  (see Paper I), the inference that the CO instability is responsible for

the 3 min oscillation would be speculative. The excitation of oscillations in the chromosphere by a thermo-convective instability was also mooted by Defouw (1970), although the physical mechanism of the instability he suggested is entirely different from ours.

The choice of our initial atmospheric model deserves some attention. This model was constructed without taking into account the presence of a magnetic field. We arbitrarily assumed that the temperature stratification, even in a flux tube, is the same as the non-magnetic region. However, we chose a lower pressure, so as to satisfy the condition for horizontal pressure balance. Such a configuration is, of course, no longer in energy equilibrium. The strong transient generated during the initial phases of the simulations are a consequence of starting with a non-equilibrium atmosphere. In general, the larger the departure of the starting configuration from equilibrium, the more pronounced is the transient behaviour. After sufficient time, the atmosphere should ordinarily relax to a new equilibrium state. Owing to the CO instability, which is not quenched, even in the presence of a magnetic field, the final state is not a steady one, but an oscillating one. The oscillations are driven overstable by the radiation field. We find that for strong dynamic effects to occur, the magnetic field strength in the tube should not be too large. For example we find that in the final state,  $B \sim 50\text{--}100\text{ G}$  at  $z = 500\text{ km}$  and  $B \sim 600\text{ G}$  at  $z = 80\text{ km}$ . These values probably fall short of those observed in the photosphere, below the chromosphere network region (Stenflo, 1989 and references therein; Muller, 1985; but see also Semel, 1986). It might be possible that the field strengths that we have considered occur either during the birth and decay phases of flux elements, on a time scale of some 1000 s (Hasan, 1985; Schüssler, 1989) or in 'weak field' elements outside the chromospheric network. Also in the present investigation, we dealt with a single magnetic element, while in reality the chromosphere is likely to be a collection of many elements. Consequently, the magnetic field is likely to be stronger in higher layers where the dynamic processes will be confined laterally, so that the energy does not spread out. We, however, defer these points to a future paper.

As far as the computational aspect of the dynamic simulations is concerned, the FCT code with radiative transfer proved to be very stable and robust. We could, for example, follow several thousand time steps without any numerical limitation. In practice, it was found that 1000 time steps sufficed to explain the essential features associated with the nonlinear development of the CO instability. Also, observations of network bright points by Muller (1983) suggest a limited lifetime  $\approx 20\text{ min}$  for the small-scale magnetic elements.

Lastly, we would briefly like to comment on the use of the thin flux tube approximation. This approximation was made for mathematical convenience. As already pointed out, it is unlikely to hold in the upper layers of the tube, where its radius exceeds the local pressure height. Using a 2D or 3D approach would, of course, be more accurate. However, although this would change the details of the results, the essential aspects to emerge from our calculations are likely to remain unmodified.

*Acknowledgements.* We thank Drs. M. Knölker, D. Schmitt and J. Trujillo Bueno for helpful discussions and also for providing computational assistance. One of us (S.S.H) is grateful to the Alexander von Humboldt Foundation for providing financial support during his visit to Göttingen. The calculations were

carried out on the IBM 3090/300 computer of the Gesellschaft für Wissenschaftliche Datenverarbeitung, Göttingen.

## References

- Anderson, L.S.: 1989, *Astrophys. J.* **339**, 558  
 Anderson, L.S., Athay, R.G.: 1989, *Astrophys. J.* **336**, 1089  
 Athay, R.G., White, O.R.: 1978, *Astrophys. J.* **226**, 1135  
 Ayres, T.R.: 1981, *Astrophys. J.* **244**, 1064  
 Ayres, R.R., Testerman, L., Brault, J.W.: 1986, *Astrophys. J.* **304**, 542  
 Boris, J.P., Book, D.L.: 1976, *J. Comput. Phys.* **20**, 397  
 Courant, R., Friedrichs, K.: 1948, *Supersonic flow and shock waves*, Interscience, New York  
 Cram, L.: 1974, in *Chromospheric Fine Structure*, ed. R.G. Athay, Reidel, Dordrecht, p. 51  
 Defouw, R.J.: 1970, *Solar Phys.* **14**, 42  
 Defouw, R.J.: 1976, *Astrophys. J.* **209**, 266  
 Hasan, S.S., Venkatakrisnan, P.: 1980, *Kodaikanal, Obs. Bull. Ser. A* **3**, 6  
 Hasan, S.S.: 1984, *Astrophys. J.* **285**, 851  
 Hasan, S.S.: 1985, *Astron. Astrophys.* **143**, 39  
 Hasan, S.S.: 1986, *Monthly Notices Roy. Astron. Soc.* **219**, 357  
 Hasan, S.S., Kneer, F.: 1986, *Astron. Astrophys.* **158**, 288  
 Hasan, S.S.: 1989, in *Physics of Magnetic Flux Ropes*, eds. E.R. Priest, C.T. Russell, AGU Monograph (in press)  
 Kalkofen, W.: 1989, in *Solar Photosphere: Structure, Convection and Magnetic Fields*, ed. J.O. Stenflo, Kluwer, Dordrecht, p. 185  
 Kneer, F., Mattig, W.: 1978, *Astron. Astrophys.* **65**, 17  
 Kneer, F.: 1983, *Astron. Astrophys.* **128**, 311  
 Kneer, F.: 1984, in *Small Scale Dynamical Processes in Quiet Stellar Atmospheres*, ed. S.L. Keil, National Solar Obs., Sunspot, p. 110  
 Kneer, F.: 1985, in *Chromospheric Diagnostics and Modelling*, ed. B. Lites, National Solar Obs., Sunspot, p. 252  
 Kneer, F.: 1986, in *Small Scale Magnetic Flux Concentrations in the Solar Photosphere*, eds. W. Deinzer, M. Knölker, H.H. Voigt, Vandenhoek and Ruprecht, Göttingen, p. 147  
 Kneer, F., von Uexküll, M.: 1986, *Astron. Astrophys.* **155**, 178  
 Liu, S.Y.: 1974, *Astrophys. J.* **189**, 359  
 Mauas, P.J., Avrett, E.H., Loeser, R.: 1989, *Astrophys. J.* (in press)  
 Mihalas, D.: 1978, *Stellar Atmospheres*, 2nd edn., Freeman, San Francisco  
 Muchmore, D.O.: 1986, *Astron. Astrophys.* **155**, 172  
 Muchmore, D.O., Nuth III, J.A., Stencel, R.A.: 1987, *Astrophys. J.* **315**, L141  
 Muchmore, D.O., Kurucz, R.L., Ulmschneider, P.: 1988, *Astron. Astrophys.* **201**, 138  
 Muller, R.: 1983, *Solar Phys.* **85**, 113  
 Muller, R.: 1985, *Solar Phys.* **100**, 237  
 Musielak, Z.E., Rosner, E., Ulmschneider, P.: 1987, in *Cool Stars, Stellar Systems and the Sun*, eds. J.L. Linsky, R.E. Stencel, Springer, Berlin, Heidelberg, New York, p. 66  
 Musielak, Z.E., Rosner, E.: 1987, *Astrophys. J.* **315**, 371  
 Musielak, Z.E., Rosner, E.: 1988, *Astrophys. J.* **329**, 376  
 Musielak, Z.E., Rosner, E., Ulmschneider, P.: 1989, *Astrophys. J.* **337**, 470  
 Orrall, F.Q.: 1966, *Astrophys. J.* **143**, 917  
 Roberts, B., Webb, A.R.: 1978, *Solar Phys.* **56**, 5

- Schüssler, M.: 1989, in *Solar Photosphere: Structure, Convection and Magnetic Fields*, ed. J.O. Stenflo, Kluwer, Dordrecht, p. 161
- Secchi, P.A.S.J.: 1877, *Le Soleil*, Vol. 2, 2nd edn., Gauthier-Villars, Paris.
- Semel, M.: 1986, in *Small Scale Magnetic Flux Concentrations in the Solar Photosphere*, eds. W. Deinzer, M.Knölker, H.H. Voigt, Vandenhoeck and Ruprecht, Göttingen, p. 39
- Spiegel, E.A.: 1957, *Astrophys. J.* **126**, 202
- Steffen, M., Muchmore, D.: 1988, *Astron. Astrophys.* **193**, 281
- Stein, R.F.: 1967, *Solar Phys.* **2**, 385
- Stein, R.F., Leibacher, J.W.: 1974, *Ann. Rev. Astron. Astrophys.* **12**, 407
- Stenflo, J.O.: 1973, *Solar Phys.* **32**, 41
- Stenflo, J.O.: 1989, *Astron. Astrophys. Rev.* **1**, 3
- Tsuji, T.: 1988, *Astron. Astrophys.* **197**, 185
- Tsuji, T.: 1989, in *Evolution of Peculiar Red Giant Stars*, eds. H.R. Johnson, B.M. Zuckerman, Cambridge Univ. Press, Cambridge (in press)
- Ulmschneider, P.: 1970, *Solar Phys.* **12**, 403
- Ulmschneider, P., Zähringer, K.: 1987, in *Cool Stars, Stellar Systems and the Sun*, eds. J.L.Linsky, R.E. Stencel, Springer, Berlin, Heidelberg, New York, p. 63
- Vernazza, J.E., Avrett, E.H., Loeser, R.: 1981, *Astrophys. J. Suppl.* **45**, 635
- von Uexküll, M., Kneer, F., Matherbe, J.M., Mein, P.: 1989, *Astron. Astrophys.* **208**, 290
- Wiehr, E.: 1978, *Astron. Astrophys.* **69**, 279